

1 **Controls on andesitic glaciovolcanism at ice-capped volcanoes from**
2 **field and experimental studies**

3 **R.P. Cole¹, J.D.L., White¹, T. Dürig^{1,2}, R. Büttner³, B. Zimanowski³, M.H. Bowman¹, C.E.**
4 **Conway⁴, G.S. Leonard⁵, L.R. Pure⁶, D.B. Townsend⁵**

5
6 ¹Geology Department, University of Otago, Dunedin, New Zealand

7 ²Institute of Earth Sciences, University of Iceland, Reykjavík, Iceland

8 ³Physikalisch Vulkanologisches Labor, Julius-Maximilians-Universität Würzburg, Würzburg,
9 Germany

10 ⁴Research Institute of Earthquake and Volcano Geology, Geological Survey of Japan, Tsukuba, Japan

11 ⁵GNS Science, Avalon, Lower Hutt, New Zealand

12 ⁶School of Geography Environment and Earth Sciences, Victoria University of Wellington,
13 Wellington, New Zealand

14

15 **ABSTRACT**

16 Glaciovolcanic deposits at Tongariro and Ruapehu volcanoes, New Zealand, represent diverse
17 styles of interaction between wet-based glaciers and andesitic lava. There are ice-confined lavas, and
18 also hydroclastic breccia and subaqueous pyroclastic deposits that formed during effusive and
19 explosive eruptions into meltwater beneath the glacier; they are rare among globally reported products
20 of andesitic glaciovolcanism. The apparent lack of hydrovolcanically fragmented andesite at ice-
21 capped volcanoes has been attributed to a lack of meltwater at the interaction sites, because either the
22 thermal characteristics of andesite limit meltwater production, or meltwater drains out through leaky
23 glaciers and down steep volcano slopes. We use published field evidence and novel, dynamic
24 andesite-ice experiments to show that, in some cases, meltwater accumulates under glaciers on
25 andesitic volcanoes, and that meltwater production rates increase as andesite pushes against an ice
26 wall. We concur with models for eruptions beneath ice sheets that the glacial conditions and pre-
27 eruption edifice morphology are more important controls on the style of glaciovolcanism and its
28 products than magma composition and the thermal properties of magmas. Glaciovolcanic products
29 can be useful proxies for paleoenvironment, and the range of andesitic products and the hydrological
30 environments in which andesite erupts is greater than hitherto appreciated.

31

32 **INTRODUCTION**

33 Currently, 254 Holocene volcanoes host glacial ice, 72% of which are arc volcanoes, and
34 numerous high latitude and high altitude intermediate-composition (hereafter termed “andesitic”)

35 stratovolcanoes were glaciated during the Plio-Pleistocene (Edwards et al., 2020). Ice-confined lava
36 is a well-documented product of andesitic glaciovolcanism, formed when a glacier physically
37 confines lava to high interfluves; little to no hydrovolcanic fragmentation takes place (e.g., Lescinsky
38 and Fink, 2000; Kelman et al., 2002; Conway et al., 2015). The rarity of reported andesitic
39 glaciovolcanic clastic products (Kelman et al., 2002) has been taken to indicate that fragmentation is
40 rare at glaciated arc volcanoes. Lower eruption temperatures have been suggested to reduce the rate
41 of ice-melting for intermediate-silicic lavas compared with basalts, so that meltwater is driven out by
42 by positive pressures in the englacial vault, impeding hydrovolcanic fragmentation (Höskuldsson and
43 Sparks, 1997; Kelman et al., 2002; c.f. Stevenson et al., 2009). No observational or experimental data
44 have been published, however, to support an entirely compositional control on a lava's ability to melt
45 ice. Field observations and experiments with basaltic lava show that ice melting rates increase when
46 flow or inflation rate is low, and that melting is faster when lava directly contacts ice, rather than
47 snow or a carapace of breccia (Edwards et al., 2013, 2015). The only experiments to date with broadly
48 andesitic melts show heat fluxes similar to basalts (Oddsson et al., 2016b). Low calculated heat fluxes
49 and a lack of subaqueous deposits at the Table, an andesitic lava-dominated tuya in British Columbia,
50 were explained by low effusion rates, a carapace of insulating breccia and meltwater drainage on
51 steep slopes (Wilson et al., 2019). In addition, the range of clastic and coherent glaciovolcanic
52 products from basaltic and rhyolitic volcanoes indicates production of varied volumes of meltwater
53 by both magma types (e.g., Smellie and Skilling, 1994; Stevenson et al., 2006; Tuffen et al., 2008;
54 McGarvie, 2009; Smellie, 2018). The apparent lack of hydroclastic rocks at many andesitic edifices
55 arguably results from poor meltwater retention at arc volcanoes, due to steep terrain, and thin,
56 permeable glaciers (Lescinsky and Fink, 2000; Stevenson et al., 2009). There are far fewer published
57 studies of andesitic glaciovolcanism than for basalt and rhyolite. Also, volcanoclastic products from
58 explosive eruptions that land on snow or ice of a cone's slopes are not preserved on the edifice,
59 leading to a preservation and publication bias towards ice-confined lavas (Kelman et al., 2002).

60 We identify distinct styles of glaciovolcanism at andesitic volcanoes capped by wet-based
61 glaciers using evidence published from Tongariro and Ruapehu volcanoes, New Zealand (Conway et
62 al., 2015, 2016; Cole et al., 2018, 2020). The examples given represent styles of glaciovolcanism that
63 may have occurred at many ice-capped andesitic edifices worldwide, and there is also overlap with
64 volcano-ice interactions under large ice sheets (e.g., Stevenson et al., 2009).

65 New molten andesite-ice deformation experiments, building on static experiments by Oddsson
66 et al. (2016b), tested rates of heat flux and meltwater production during dynamic lava-ice interaction.
67 Active pushing of lava against ice has not been considered before, but it probably occurs in most
68 natural lavas as they flow or inflate against an ice barrier or roof. Our results suggest this dynamic
69 influence on the heat transfer is significant. Understanding the thermodynamics of intermediate-

70 composition lava-ice interaction is important for assessing emplacement of glaciovolcanic products,
71 and for forecasting whether meltwater may cause flooding and/or influence explosive activity (Major
72 and Newhall, 1989; Lescinsky and Fink, 2000).

73

74 **STYLES OF ANDESITIC GLACIOVOLCANISM**

75 Three types of glaciovolcanic product are preserved on Tongariro and Ruapehu (Fig 1; Conway
76 et al., 2015; Townsend et al., 2017; Cole et al., 2018, 2020), recording diverse glaciovolcanic styles
77 from magmas of similar composition. Approximately 90% of analysed lavas from Ruapehu are
78 basaltic-andesite or andesite (Price et al., 2012; Conway et al., 2016), and 77% of visible, edifice-
79 forming units at Tongariro are andesite, while 23% are basaltic-andesite (Pure et al., 2020).
80 Temperatures of most historic eruptions at Ruapehu have been estimated at 950 to 1050 °C (Kilgour
81 et al., 2013). Russell et al. (2014) defined 9 types of tuya based on eruption style and glacio-
82 hydrological conditions, all independent of magma composition. On a smaller scale, we suggest that
83 different glacio-hydrological conditions on an ice-capped volcano can yield at least three distinct
84 glaciovolcanic products from three pairings of eruptive style with environmental conditions (Fig. 2):

85 1) ***Effusive and subaqueous.*** Effusive eruptions into ponded water lead to non-explosive,
86 quench fragmentation forming massive hyalo-/hydroclastic breccias (Fig. 1 A and B; Cole et al.,
87 2020). Meltwater accumulation has led to similar deposits at volcanoes in large ice sheets across the
88 range of magma compositions (e.g., Smellie and Skilling, 1994; McGarvie et al., 2007; Stevenson et
89 al., 2009). In glacial periods, multi-vent composite volcanoes have supported glaciers a few hundred
90 metres thick within valleys, or on an irregular summit topography (Eaves et al., 2016; Cole et al.,
91 2018, 2020). Thick ice combined with confining topography enables meltwater to pond locally even
92 at generally steep-sided volcanoes, influencing glaciovolcanic interaction (Fig. 2).

93 2) ***Explosive and subaqueous.*** Deposits of aqueous pyroclastic currents formed from explosive
94 eruptions into meltwater (Figs. 1C, D and 2). They were emplaced either by meltwater draining
95 through a subglacial channel, or by currents moving through accumulated water, such as an englacial
96 lake; deposition from eruption-fed currents in either setting produces similar features, but with
97 different implications for glacial hydrology (Smellie and Skilling, 1994; White, 2000). Based on the
98 surrounding topography at Tongariro, the deposits are inferred to have been emplaced in meltwater
99 channels along an ice-capped ridgeline (ice \leq 150 m thick; Fig. 2; Cole et al., 2018). Comparable
100 deposits formed in Iceland where ice $>$ 550 m thick is inferred to have overwhelmed topography
101 (Stevenson et al., 2009).

102 3) ***Effusive and ice-confined.*** Ridge-capping lava flows formed from effusive eruptions, but
103 represent a different style of glaciovolcanism to hydroclastic breccia. Their over-thickened forms and
104 the orientation of marginal cooling joints indicate that lava was physically confined by the glacier

105 (Fig. 1 E and F). Meltwater is produced and contributes to cooling and fracturing in these settings,
106 but the lavas are not emplaced in ponded water. At Tongariro and Ruapehu (Conway et al., 2015;
107 Cole et al., 2018), and other stratovolcanoes globally (Lescinsky and Sisson, 1998; Lescinsky and
108 Fink, 2000), ice-confined lavas are perched at high elevations on steep terrain. They erupted alongside
109 thin, fractured alpine glaciers that allowed meltwater to drain freely from the site of interaction. In
110 ice sheets, lava-dominated products cap edifices that became emergent, or form entire edifices where
111 glacial conditions permit efficient drainage (Smellie and Skilling, 1994; Tuffen et al., 2002;
112 Stevenson et al., 2006; Russell et al., 2014; Wilson et al., 2019).

113 The distinct deposit types (1-3) represent andesitic lava-ice interaction under different
114 hydrological conditions on ice-capped volcanoes, but there is considerable overlap with products at
115 basaltic and rhyolitic edifices, and also beneath thick ice sheets (Smellie and Skilling, 1994;
116 Stevenson et al., 2006, 2009; Tuffen et al., 2008; McGarvie, 2009; Russell et al., 2014; Smellie,
117 2018). We concur that glaciovolcanic interaction at ice-capped volcanoes is controlled by meltwater
118 availability and glacial hydrology, as functions of the glacier characteristics and edifice morphology
119 (Fig. 2).

120

121 **MOLTEN ANDESITE-ICE DEFORMATION EXPERIMENTS**

122 We conducted novel experiments to investigate how much meltwater can be produced when
123 andesitic lava flows against a glacier. We selected < 5 kyr lava (Conway et al., 2016; Townsend et
124 al., 2017) in Ruapehu's Whangaehu Valley for its apparent freshness. X-Ray Fluorescence analysis
125 (University of Waikato) confirms an andesitic composition (60 wt% SiO₂ and 5.1 wt% Na₂O+K₂O
126 with LOI at -0.15; full major element data in Data Repository). For each experiment, we melted 60-
127 100 g of granulated andesite in a crucible at 1250 °C using an induction furnace. The experimental
128 melt temperature higher than that of erupting andesite ($T \approx 1000$ °C; (Harris and Rowland, 2015))
129 counterbalances the loss of viscosity-reducing volatiles by outgassing during emplacement of the
130 natural lava (Zimanowski et al., 1991). This overheating precludes direct comparison of ice-melt rates
131 with those during emplacement of natural andesite, but it allowed the andesite to be deformed against
132 ice, which is the focus of these experiments. Despite the high melt temperature, the andesite was
133 much more viscous than remelted basalt. A squeeze apparatus was designed comprising two wooden
134 paddles attached to scissored arms. The andesite melt was pressed against an ice block frozen to one
135 of the paddles, and pressure sensors attached to the arms of the apparatus recorded the pressure
136 applied during deformation (Fig. 3A). A calorimeter beneath collected meltwater. Water mass and
137 temperature were measured during the experiments. Two additional experimental runs were
138 performed with andesite melt placed on top of an ice block, one resting under gravity only, and the

139 other being pushed into the ice (Fig. 3B). For these runs, only the mass of the meltwater was
140 measured.

141 The molten andesite was easily squeezed against the ice block, melting a cavity in the ice that
142 was only slightly wider than the andesite and of comparable shape. A widening glassy crust
143 progressed across the melt sample from the margin in direct contact with the ice, while meltwater
144 drained down from the andesite-ice interface. During the runs in which the molten andesite was
145 placed on top of an ice block, a cavity formed beneath the andesite and partially filled with meltwater.
146 The meltwater formed a channel that breached the edge of the ice block seconds after the start of the
147 experiment and ran down the side, carving a vertical chute. Some meltwater refroze to the ice before
148 reaching the calorimeter, but the majority was collected. Details of experimental procedure and heat
149 flux calculations are in the Data Repository.

150

151 The overall heat fluxes from each experiment were between 186 and 250 kW m⁻², consistent
152 with published observational and experimental values obtained for andesitic lava from
153 Eyjafjallajökull, Iceland (Oddsson et al., 2016a, 2016b) and basaltic lava effusions (Allen, 1980;
154 Höskuldsson and Sparks, 1997; Edwards et al., 2013). The fluxes are much lower than the 500-600
155 kW m⁻² estimated during the 1996 Gjálp eruption (Gudmundsson, 2003), and an order of magnitude
156 lower than the 1-4 MW m⁻² estimated from ice melting during the explosive phase of the 2010
157 Eyjafjallajökull eruption (Magnússon et al., 2012). This difference is expected because virtually no
158 fragmentation took place during the experiments. Our calculated heat fluxes are higher than those
159 calculated for the emplacement of the Table in British Columbia, where endogenous emplacement
160 within an enclosing carapace of breccia is inferred to have insulated the hot interior from surrounding
161 ice (Wilson et al., 2019). We note that unlike a natural lava flow, the volume of andesite in the
162 experiments was small and not replenished by continued feeding from a vent. More fragmentation
163 would be expected in a natural lava as it cools, forms a crust, and is fractured by quenching and
164 dynamic stressing. Heat transfer and meltwater production would be prolonged by continued feeding.
165 If issues associated with the high viscosity of remelted andesite can be overcome, large-scale
166 experiments with greater volumes of melt that remain molten for longer (e.g., Edwards et al., 2013)
167 to determine heat transfer while measuring flow or strain rate would provide results more easily
168 scalable to natural lava emplacement in ice.

169 Our attempt to recreate the dynamic interaction between ice and deforming lava produced
170 transient increases in heat flux of up to an order of magnitude, following increases in applied force,
171 causing temporary rises in meltwater production (Fig. 3A). Compared with static molten andesite-ice
172 interaction, meltwater was produced at a higher rate and in greater volume when the andesite melt
173 was pressed into the ice (Fig. 3B). The increases in heat flux and meltwater production from

174 deforming melt are inferred to result from advection of heat to the melt-ice interface, an increased
175 interface area from lateral spreading of the deforming melt, and the formation of cracks in the
176 solidifying andesite due to the applied force. The offset in time of a few seconds between increase in
177 applied force and increase in meltwater production is expected due to the time taken for ice melting,
178 the fall of the meltwater into the calorimeter and the delay in mass recording due to inertia of the
179 balance. Overall results from additional experimental runs and the limitations of our experimental
180 procedure, which could be developed further, are given in the Data Repository.

181 We find that meltwater production increases when lava flows, or inflates, against a glacier, as
182 would occur during emplacement of ice-confined lava of any composition. An area where the
183 deformation simulated in these experiments is likely to be most significant is at the flow front of a
184 lava, where it presses against the glacier with the force of the remaining flow behind it. The effect on
185 meltwater production from dynamic lava-ice interaction should be included in theoretical and
186 experimental models to fully understand the ice-melting potential of different lavas. Lava flow rate,
187 contact area and contact geometry with ice, and the rate and geometry of surface crust fracturing
188 during flow or extrusion, as well as the ability of meltwater to drain away, are probably more
189 important than magma composition in controlling glaciovolcanic interaction style and products.

190

191 **CONCLUSION**

192 Andesite is able to generate enough meltwater during eruptions at ice-capped volcanoes to form
193 subaqueous lithofacies. Further, heat transfer and meltwater production increase during dynamic
194 interactions when lava flows or inflates against glacial ice. The dynamic effect should be considered
195 in models for meltwater production from ice-confined lava, and large-scale experiments undertaken
196 to better quantify this effect. The dominance of ice-confined lavas in known intermediate-
197 composition glaciovolcanic sequences probably reflects preservation bias or meltwater drainage in
198 leaky systems. Meltwater retention controlled by glacial hydrology plays a more significant role in
199 volcano-ice interaction style than compositionally controlled differences in rates of meltwater
200 production.

201

202 **ACKNOWLEDGEMENTS**

203 RPC received funding from the Geological Society of New Zealand Wellman Research Award
204 and the University of Otago Polar Environments Research Theme. The Department of Conservation
205 provided logistical assistance in the field. Brent Pooley and Luke Easterbrook assisted with making
206 the experimental apparatus. Matteo Demurtas helped RPC in using MatLab. Kelly Russell, John
207 Smellie, and Alison Graettinger provided constructive reviews.

208

209 **FIGURES AND CAPTIONS**

210

211 **Figure 1:** Glaciovolcanic products preserved at Tongariro and Ruapehu volcanoes. Massive,
212 hydroclastic breccia with quench fragmentation textures at Ruapehu (A) and Tongariro (B). C and D:
213 a well-sorted, bedded subaqueous pyroclastic current deposit with traction structures. E and F: Ice-
214 confined, subglacial lava flows inferred to have tunnelled through and cooled within Ruapehu valley
215 glaciers, since retreated.

216 **Figure 2:** Schematic diagram showing the inferred glacial and edifice characteristics for each type of
217 glaciovolcanic product preserved at Tongariro and Ruapehu pictured in Figure 1. 1: Fig. 1 E and F;
218 Conway et al. (2015); 2: Fig. 1 C and D; Cole et al. (2018) 3: Fig. 1 A and B; Cole et al. (2020).

219 **Figure 3:** A and B: Dynamic experiment setup. (A) includes heat flux and meltwater production
220 curves from one experiment shown in relation to applied force with time. Applied force is shown
221 qualitatively in arbitrary units (a.u.). (B) shows meltwater accumulation during dynamic interaction
222 compared to static.

223

224 **REFERENCES CITED**

- 225 Allen, C.C., 1980, Icelandic subglacial volcanism: thermal and physical studies.: *Journal of*
226 *Geology*, v. 88, p. 108–117, doi:10.1086/628478.
- 227 Cole, R.P., White, J.D.L., Conway, C.E., Leonard, G.S., Townsend, D.B., and Pure, L.R., 2018,
228 The glaciovolcanic evolution of an andesitic edifice, South Crater, Tongariro volcano, New
229 Zealand: *Journal of Volcanology and Geothermal Research*, v. 352, p. 55–77,
230 doi:10.1016/j.jvolgeores.2017.12.003.
- 231 Cole, R.P., White, J.D.L., Townsend, D.B., Leonard, G.S., and Conway, C.E., 2020, Glaciovolcanic
232 emplacement of an intermediate hydroclastic breccia-lobe complex during the penultimate
233 glacial period (190 – 130 ka), Ruapehu volcano, New Zealand: *Geological Society of America*
234 *Bulletin*, doi:10.1130/B35297.1.
- 235 Conway, C.E., Leonard, G.S., Townsend, D.B., Calvert, A.T., Wilson, C.J.N., Gamble, J.A., and
236 Eaves, S.R., 2016, A high-resolution $^{40}\text{Ar}/^{39}\text{Ar}$ lava chronology and edifice construction
237 history for Ruapehu volcano, New Zealand: *Journal of Volcanology and Geothermal Research*,
238 v. 327, p. 152–179, doi:10.1016/j.jvolgeores.2016.07.006.
- 239 Conway, C.E., Townsend, D.B., Leonard, G.S., Wilson, C.J.N., Calvert, A.T., and Gamble, J.A.,
240 2015, Lava-ice interaction on a large composite volcano: a case study from Ruapehu, New
241 Zealand: *Bulletin of Volcanology*, v. 77, p. 21, doi:10.1007/s00445-015-0906-2.
- 242 Eaves, S.R., Mackintosh, A.N., Anderson, B.M., Doughty, A.M., Townsend, D.B., Conway, C.E.,
243 Winckler, G., Schaefer, J.M., Leonard, G.S., and Calvert, A.T., 2016, The Last Glacial

244 Maximum in the central North Island, New Zealand: Palaeoclimate inferences from glacier
245 modelling: *Climate of the Past*, v. 12, p. 943–960, doi:10.5194/cp-12-943-2016.

246 Edwards, B.R., Belousov, A., Belousova, M., and Melnikov, D., 2015, Observations on lava,
247 snowpack and their interactions during the 2012–13 Tolbachik eruption, Klyuchevskoy Group,
248 Kamchatka, Russia: *Journal of Volcanology and Geothermal Research*, v. 307, p. 107–119.

249 Edwards, B.R., Karson, J., Wysocki, R., Lev, E., Bindeman, I., and Kueppers, U., 2013, Insights on
250 lava-ice/snow interactions from large-scale basaltic melt experiments: *Geology*, v. 41, p. 851–
251 854, doi:10.1130/G34305.1.

252 Edwards, B., Kochtitzky, W., and Battersby, S., 2020, Global mapping of future glaciovolcanism:
253 *Global and Planetary Change*, doi:10.1016/j.gloplacha.2020.103356.

254 Gudmundsson, M.T., 2003, Melting of ice by magma-ice-water interactions during subglacial
255 eruptions as an indicator of heat transfer in subaqueous eruptions: *Geophysical Monograph*
256 *Series*, v. 140, p. 61–72, doi:10.1029/140GM04.

257 Harris, A.J.L., and Rowland, S.K., 2015, Lava Flows and Rheology: *Encyclopedia of Volcanoes*, p.
258 321–342.

259 Höskuldsson, A., and Sparks, R.S.J., 1997, Thermodynamics and fluid dynamics of effusive
260 subglacial eruptions: *Bulletin of Volcanology*, v. 59, p. 219–230, doi:10.1007/s004450050187.

261 Kelman, M.C., Russell, J.K., and Hickson, C.J., 2002, Effusive intermediate glaciovolcanism in the
262 Garibaldi Volcanic Belt, southwestern British Columbia, Canada (J. L. Smellie & M. G.
263 Chapman, Eds.): *Geological Society, London, Special Publications*, v. 202, p. 195–211.

264 Kilgour, G., Blundy, J., Cashman, K., and Mader, H.M., 2013, Small volume andesite magmas and
265 melt-mush interactions at Ruapehu, New Zealand: Evidence from melt inclusions:
266 *Contributions to Mineralogy and Petrology*, v. 166, p. 371–392, doi:10.1007/s00410-013-
267 0880-7.

268 Lescinsky, D.T., and Fink, J.H., 2000, Lava and ice interaction at stratovolcanoes: Use of
269 characteristic features to determine past glacial extents and future volcanic hazards: *Journal of*
270 *Geophysical Research: Solid Earth*, v. 105, p. 23711–23726, doi:10.1029/2000jb900214.

271 Lescinsky, D.T., and Sisson, T.W., 1998, Ridge-forming, ice-bounded lava flows at Mount Rainier,
272 Washington: *Geology*, v. 26, p. 351–354, doi:10.1130/0091-
273 7613(1998)026<0351:RFIBLF>2.3.CO;2.

274 Magnússon, E., Gudmundsson, M.T., Roberts, M.J., Sigurðsson, G., Höskuldsson, F., and Oddsson,
275 B., 2012, Ice-volcano interactions during the 2010 Eyjafjallajökull eruption, as revealed by
276 airborne imaging radar: *Journal of Geophysical Research: Solid Earth*, v. 117,
277 doi:10.1029/2012JB009250.

278 Major, J.J., and Newhall, C.G., 1989, Snow and ice perturbation during historical volcanic

279 eruptions and the formation of lahars and floods - A global review: *Bulletin of Volcanology*, v.
280 52, p. 1–27, doi:10.1007/BF00641384.

281 McGarvie, D., 2009, Rhyolitic volcano-ice interactions in Iceland: *Journal of Volcanology and*
282 *Geothermal Research*, v. 185, p. 367–389, doi:10.1016/j.jvolgeores.2008.11.019.

283 McGarvie, D.W., Stevenson, J.A., Burgess, R., Tuffen, H., and Tindle, A.G., 2007, Volcano-ice
284 interactions at Prestahnúkur, Iceland: Rhyolite eruption during the last interglacial-glacial
285 transition: *Annals of Glaciology*, v. 45, p. 38–47, doi:10.3189/172756407782282453.

286 Oddsson, B., Gudmundsson, M.T., Edwards, B.R., Thordarson, T., Magnússon, E., and Sigurðsson,
287 G., 2016a, Subglacial lava propagation, ice melting and heat transfer during emplacement of
288 an intermediate lava flow in the 2010 Eyjafjallajökull eruption: *Bulletin of Volcanology*, v. 78,
289 doi:10.1007/s00445-016-1041-4.

290 Oddsson, B., Gudmundsson, M.T., Sonder, I., Zimanowski, B., and Schmid, A., 2016b,
291 Experimental studies of heat transfer at the dynamic magma ice/water interface: Application to
292 subglacially emplaced lava: *Journal of Geophysical Research: Solid Earth*, v. 121, p. 3261–
293 3277.

294 Price, R.C., Gamble, J.A., Smith, I.E.M., Maas, R., Waight, T., Stewart, R.B., and Woodhead, J.,
295 2012, The anatomy of an andesite volcano: A time-stratigraphic study of andesite petrogenesis
296 and crustal evolution at Ruapehu Volcano, New Zealand: *Journal of Petrology*, v. 53, p. 2139–
297 2189, doi:10.1093/petrology/egs050.

298 Pure, L.R., Leonard, G.S., Townsend, D.B., Wilson, C.J.N., Calvert, A.T., Cole, R.P., Conway,
299 C.E., Gamble, J.A., and Smith, T. ‘Bubs,’ 2020, A high resolution $^{40}\text{Ar}/^{39}\text{Ar}$ lava chronology
300 and edifice construction history for Tongariro volcano, New Zealand: *Journal of Volcanology*
301 *and Geothermal Research*, v. 403, p. 106993, doi:10.1016/j.jvolgeores.2020.106993.

302 Russell, J.K., Edwards, B.R., Porritt, L., and Ryane, C., 2014, Tuyas: A descriptive genetic
303 classification: *Quaternary Science Reviews*, v. 87, p. 70–81,
304 doi:10.1016/j.quascirev.2014.01.001.

305 Smellie, J.L., 2018, *Glaciovolcanism: A 21st Century Proxy for Palaeo-Ice*: Elsevier Ltd, 335–375
306 p., doi:10.1016/B978-0-08-100524-8.00010-5.

307 Smellie, J.L., and Skilling, I.P., 1994, Products of subglacial volcanic eruptions under different ice
308 thicknesses: two examples from Antarctica: *Sedimentary Geology*, v. 91, p. 115–129,
309 doi:10.1016/0037-0738(94)90125-2.

310 Stevenson, J.A., McGarvie, D.W., Smellie, J.L., and Gilbert, J.S., 2006, Subglacial and ice-contact
311 volcanism at the Öreafjökull stratovolcano, Iceland: *Bulletin of Volcanology*, v. 68, p. 737–
312 752, doi:10.1007/s00445-005-0047-0.

313 Stevenson, J.A., Smellie, J.L., McGarvie, D.W., Gilbert, J.S., and Cameron, B.I., 2009, Subglacial

314 intermediate volcanism at Kerlingarfjöll, Iceland: Magma-water interactions beneath thick ice:
315 Journal of Volcanology and Geothermal Research, v. 185, p. 337–351,
316 doi:10.1016/j.jvolgeores.2008.12.016.

317 Townsend, D.B., Leonard, G.S., Conway, C.E., Eaves, S.R., and Wilson, C.J.N., 2017, Geology of
318 the Tongariro National Park Area: GNS Science Geological Map 4, p. 1 sheet + 109 pp.

319 Tuffen, H., McGarvie, D.W., Gilbert, J.S., and Pinkerton, H., 2002, Physical volcanology of a
320 subglacial-to-emergent rhyolitic tuya at Rauðufossafjöll, Torfajökull, Iceland: Geological
321 Society Special Publication, v. 202, p. 213–236, doi:10.1144/GSL.SP.2002.202.01.11.

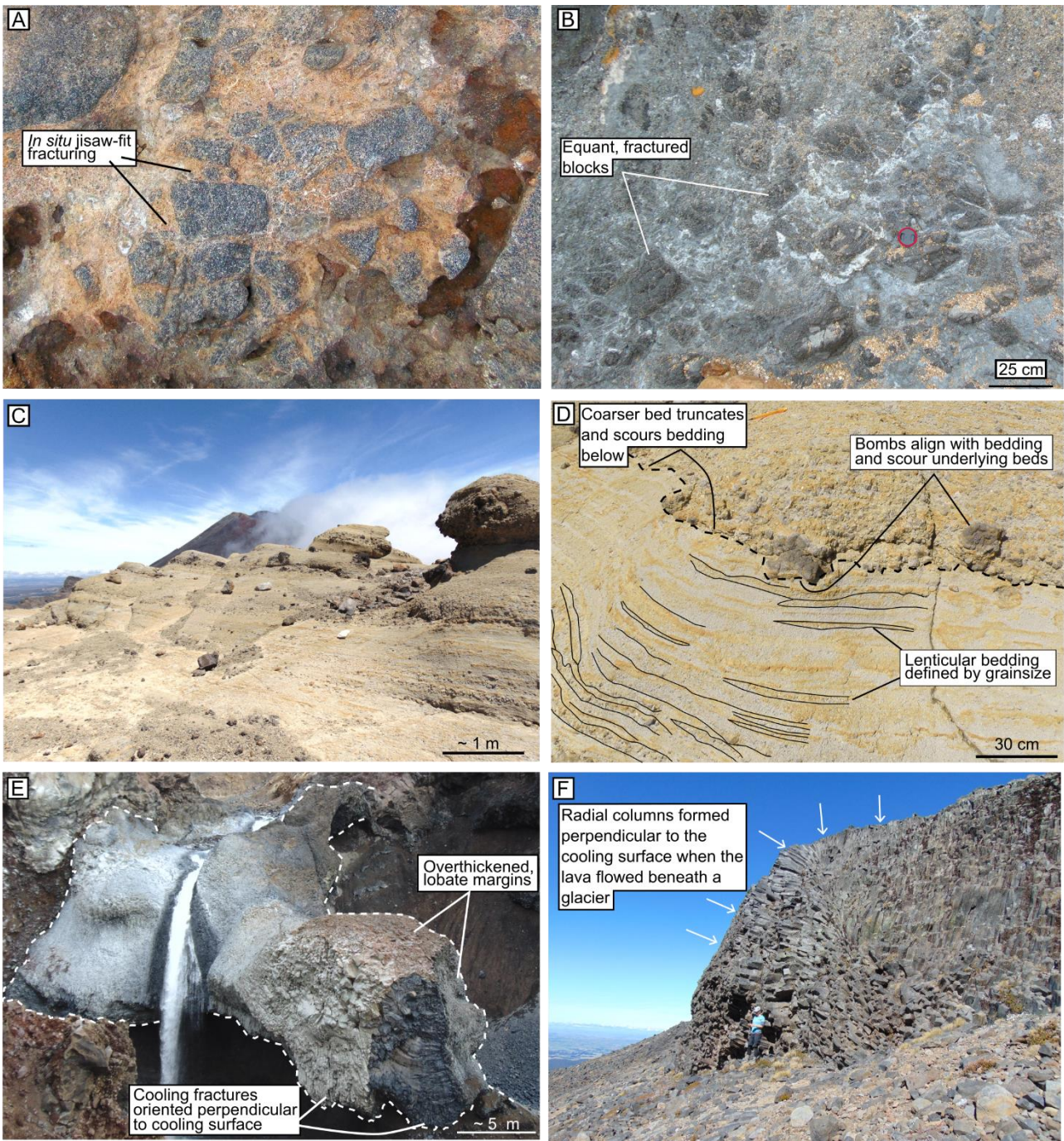
322 Tuffen, H., McGarvie, D.W., Pinkerton, H., Gilbert, J.S., and Brooker, R.A., 2008, An explosive -
323 Intrusive subglacial rhyolite eruption at Dalakvísl, Torfajökull, Iceland: Bulletin of
324 Volcanology, v. 70, p. 841–860, doi:10.1007/s00445-007-0174-x.

325 White, J.D.L., 2000, Subaqueous eruption-fed density currents and their deposits: Precambrian
326 Research, v. 101, p. 87–109, doi:10.1016/S0301-9268(99)00096-0.

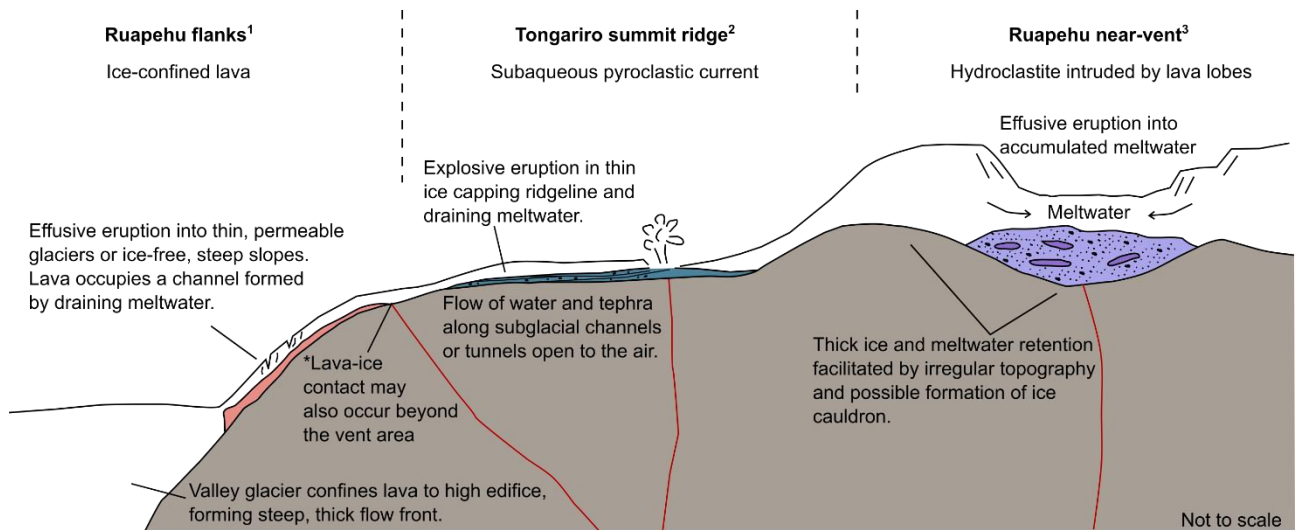
327 Wilson, A.M., Russell, J.K., and Quane, S.L., 2019, The table, a flat-topped volcano in southern
328 British Columbia: Revisited: American Journal of Science, v. 319, p. 44–73,
329 doi:10.2475/01.2019.02.

330 Zimanowski, B., Fröhlich, G., and Lorenz, V., 1991, Quantitative experiments on phreatomagmatic
331 explosions: Journal of Volcanology and Geothermal Research, v. 48, p. 341–358,
332 doi:10.1016/0377-0273(91)90050-A.

333
334



338 **Figure 1:** Glaciovolcanic products preserved at Tongariro and Ruapehu volcanoes. Massive,
 339 hydroclastic breccia with quench fragmentation textures at Ruapehu (A) and Tongariro (B). C and D:
 340 a well-sorted, bedded subaqueous pyroclastic current deposit with traction structures. E and F: Ice-
 341 confined, subglacial lava flows inferred to have tunnelled through and cooled within valley glaciers
 342 at Ruapehu, since retreated.

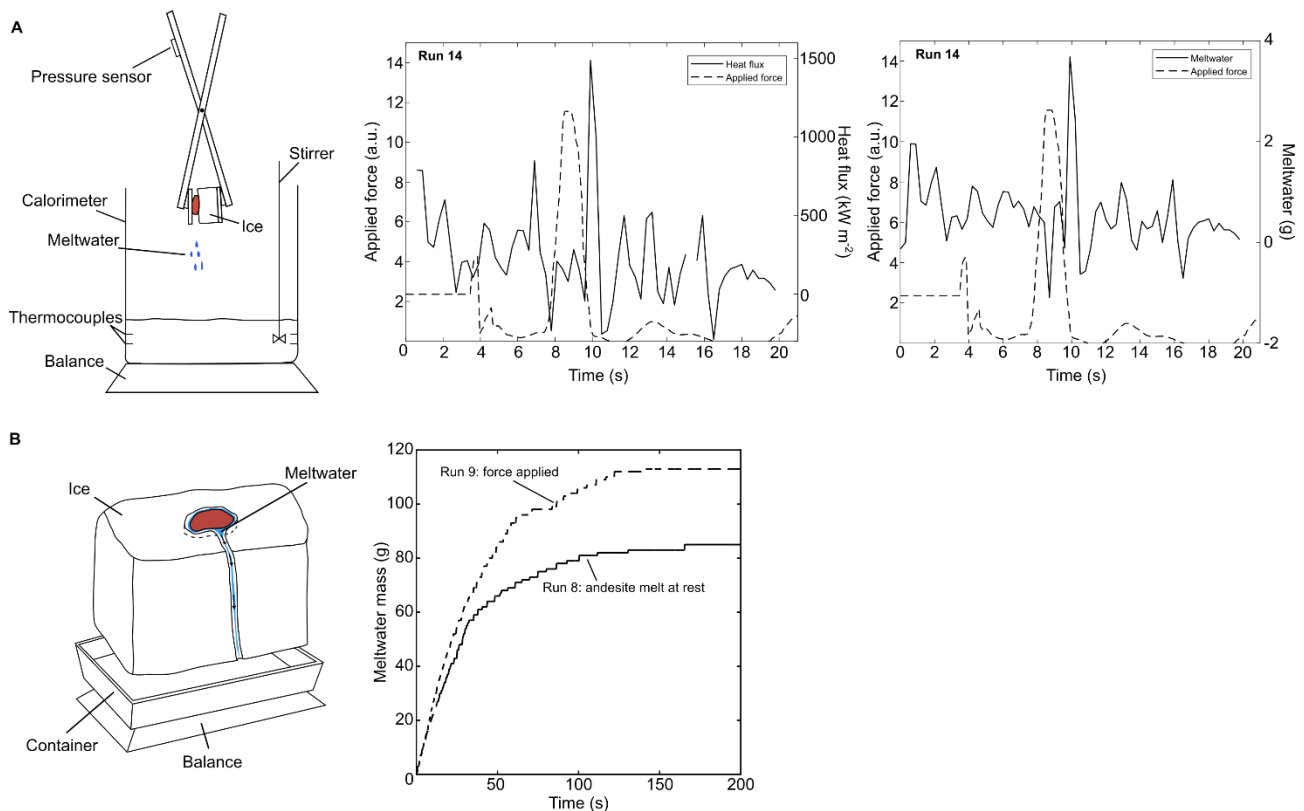


344

345

346 **Figure 2:** Schematic diagram showing the inferred glacial and edifice characteristics for each type of
 347 glaciovolcanic product preserved at Tongariro and Ruapehu pictured in Figure 1. 1: Fig. 1 E and F;
 348 Conway et al. (2015); 2: Fig. 1 C and D; Cole et al. (2018) 3: Fig. 1 A and B; Cole et al. (2020).

349



350

351

352 **Figure 3:** A and B: Experimental setup for the dynamic experiments. (A) includes heat flux and
 353 meltwater production curves from one experiment shown in relation to applied force with time.
 354 Applied force is shown qualitatively in arbitrary units (a.u.). (B) shows meltwater accumulation
 355 during dynamic interaction compared to static.

